**Supplementary Table 1: Primers used for genotyping and qRT-PCR**

| Gene | Forward Primer | Reverse Primer |
|---|---|---|
| InvtTA | AACAACCCGTAAACTCGCCC | GCAACCTAAAGTAAAATGCCCCAC |
| K14rTA | GTCGGTATCGAAGGCCTGACG | GAGAGGAGAGCACAGCGGAAT |
| TetORas | TGAAAGTCGAGCTCGGTA | GCCGGCGGTATCCAGGATGTCCAAC |
| TNFα | ACCACGCTCTTCTGTCTACT | AGGAGGTTGACTTTCTCCTG |
| IL-1β | AAGGGCTGCTTCCAAACCTTTGAC | ATACTGCCTGCCTGAAGCTCTTGT |
| IFNγ | TCTTCCTCATGGCTGTTTCTGGCT | CGCTTATGTTGTTGCTGATGGCCT |
| IL-12 | ATGACCCTGTGCCTTGGTAG | GGAGCTCAGATAGCCCATCA |
| IL-33 | GGGCTCACTGCAGGAAAGTA | TTTGCCGGGGAAATCTTGGA |
| TSLP | TGGTTCTTCTCAGGAGCCTCT | GCAGCCAGGGATAGGATTGAG |
| IL-4 | CCACGGATGCGACAAAAATCA | CTTGGAAGCCCTACAGACGAG |
| LT | ACCAGAAACTGACCTCAACCC | CGACGTGGCAGTAGAGGTAAT |
| IL-6 | AACCGCTATGAAGTTCCTCTCTGC | TAAGCCTCCGACTTGTGAAGTGGT |
| TGFβ | TGATAAGAGGGGACGGTTTG | ATTGGTGGGAGCAAAAACAG |
| IL-10 | GGGTTGCCAAGCCTTATCGGAAAT | TGGCCTTGTAGACACCTTGGTCTT |
| IL-35 | CACGGTGCCCTACATGCTAAA | GAGAGAAGATGTCCGGGAAGG |
| S100A9 | TCATCGACACCTTCCATCAA | TTACTTCCCACAGCCTTTGC |
| KC | GCTGGGATTCACCTCAAGAA | TCTCCGTTACTTGGGGACAC |
| CCL2 | TCACCTGCTGCTACTCATTCACCA | AAAGGTGCTGAAGACCTTAGGGCA |
| GM-CSF | CAAAGGGGATATCAGTCAGAAAGG | TGTGGTCTACAGCCTCTCAGCAC |
| IL-1α | TGGCCAAAGTTCCTGACTTGTTTG | CAGGCTATTTAACCAAGTGGTGCT |
| Arg1 | ACCTGGCCTTTGTTGATGTCCCTA | AGAGATGCTTCCAACTGCCAGACT |

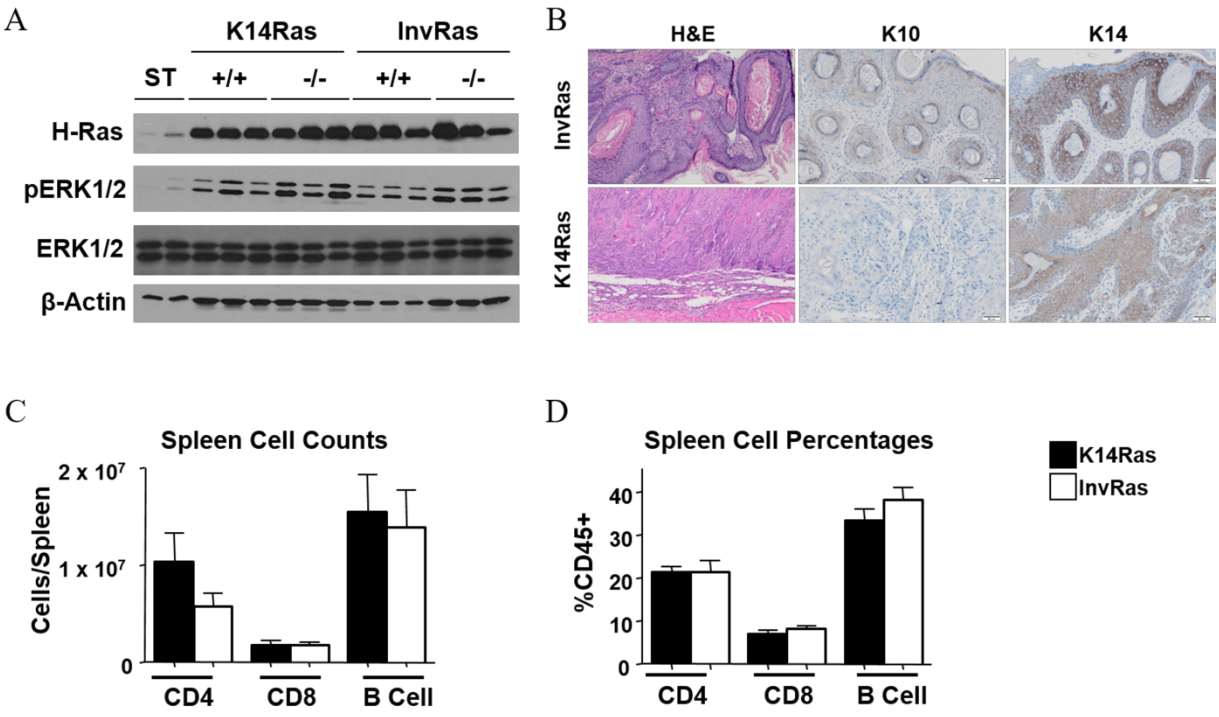


**Supplementary Figure 1:** Establishment of murine models of targeted H-Ras$^{V12G}$ to basal and suprabasal layers of the epidermis. (A) Immunoblot analysis of H-Ras, pERK1/2, ERK1/2, and β-Actin conducted on snap frozen whole tumor tissue of Single Transgenic control (ST), and *Rag1*+/+ (+/+) and *Rag1*-/- (-/-) mice of both models. (B) stained with Hematoxalin & Eosin (H&E), Keratin10, and Keratin14. H&E magnification 10x, Keratin10/14 magnification 20x. Analysis of splenic cell counts (C) and percentages (D), in K14Ras and InvRas tumor-bearing mice. Counts were determined using a Cellometer Auto T4 Cell Viability Counter (Nexcelom Bioscience), and quantified using FlowJo software. (C: n=10 per group, D: K14Ras n=30,30,27, InvRas n=30,30,30).

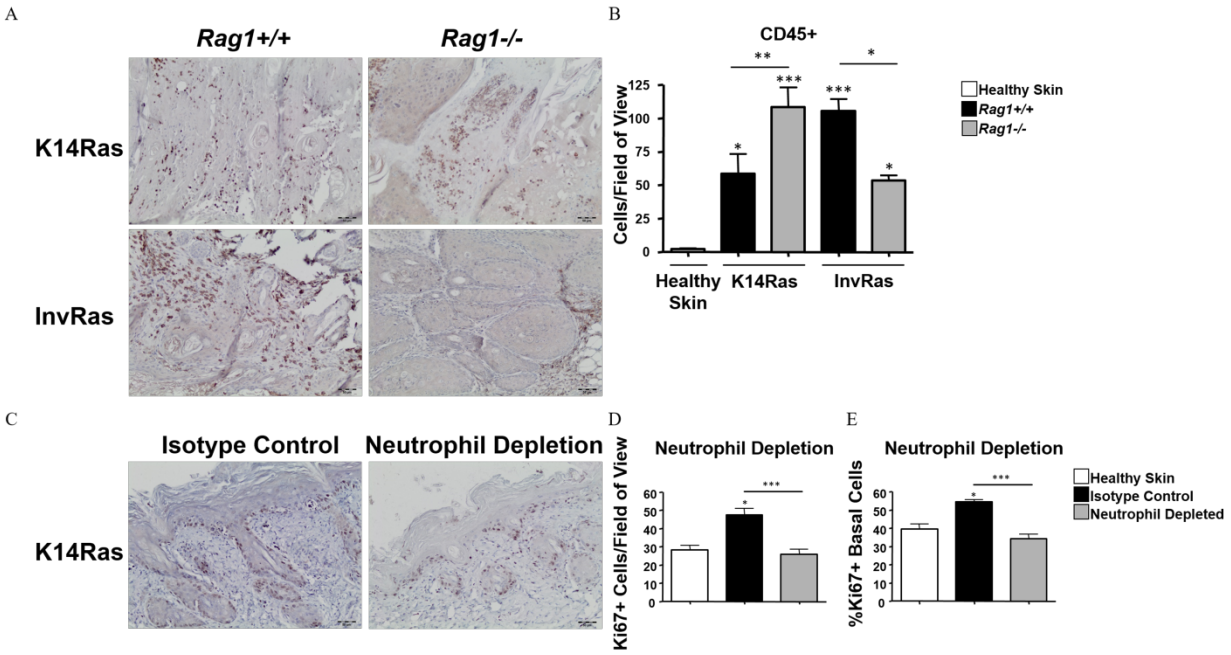


**Supplementary Figure 2:** Leukocyte infiltration into K14Ras and InvRas tumors correlates with tumor number and basal cell proliferation. Immunohistochemical analysis of CD45+ cell number and localization within tumor tissue of K14Ras and InvRas *Rag1+/+* and *Rag1-/-* (A). Magnification 20x. Average CD45+ cell counts (B) per field of view. Bars represent n=4 with 5 random fields counted (n=20). Representative immunohistochemical analysis of Ki67+ staining in hyperplastic skin of K14Ras isotype control and neutrophil depletions (C). Magnification 20x. Ki67+ basal cell number (D) and percent of total basal cells (E) quantifications. (D/E: n=5, 15, 20, 20, 20)

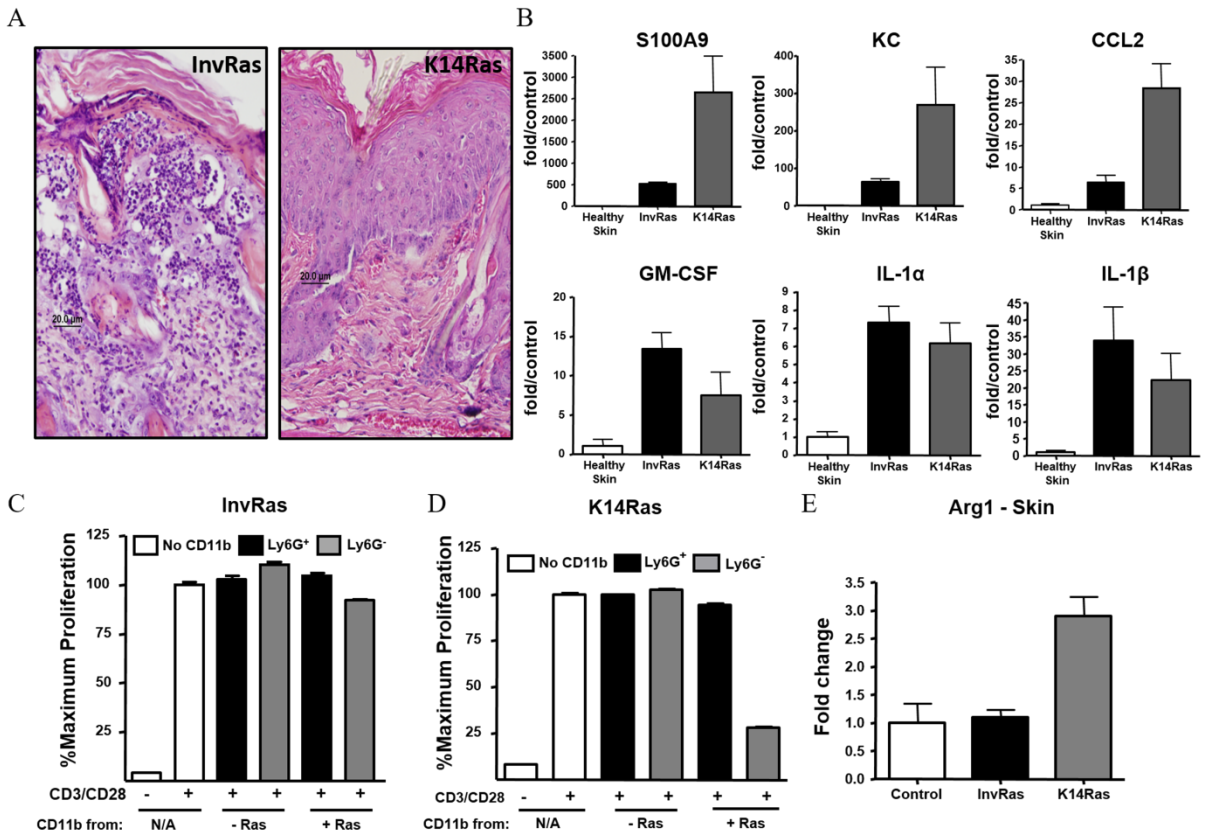


**Supplementary Figure 3:** Cytokine expression and MDSC suppression assays display distinct immunosuppressive phenotypes in K14Ras mice. Representative H&E images of K14Ras or InvRas hyperplastic skin (A). qPCR amplification of dorsal skin cDNA from healthy skin, InvRas, and K14Ras mice for the genes listed (B). (A: n=4-6 per group). Suppression assay using sorted CD11b$^{+}$ cells from spleens of InvRas (C) or K14Ras (D) mice respectively. qPCR for Arg1 transcripts in total skin from the indicated groups (E).

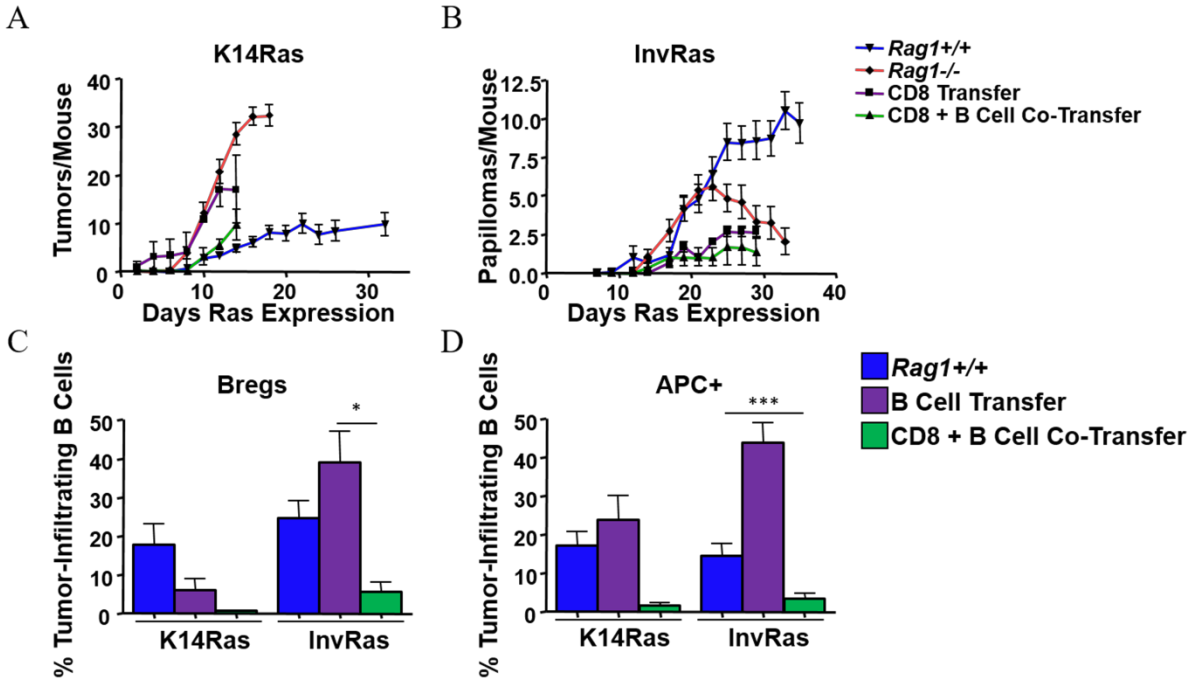


**Supplementary Figure 4:** CD8 or CD8 + B Cell transfers do not restore *Rag1*+/+ tumor counts or B cell phenotypes. Tumor counts in adoptively transferred K14Ras*Rag1*-/- (A) and InvRas*Rag1*-/- (B) mice at indicated days after Ras induction. K14Ras*Rag1*+/+, K14Ras*Rag1*-/-, InvRas*Rag1*+/+, and InvRas*Rag1*-/- mice from previous figures included as reference. (A: K14Ras*Rag1*+/+ n=45, K14Ras*Rag1*-/- n=28. CD8 Adoptive Transfer n=3, CD8 + B Cell Co-Transfer n=4. B: InvRas*Rag1*+/+ n=30, InvRas*Rag1*-/- n=27, CD8 Adoptive Transfer n=3, CD8 + B Cell Co-Transfer n=3). Analysis of tumor-infiltrating Bregs (C), and APC+ B Cells (D) in adoptive transfer experiments. (C: K14Ras*Rag1*+/+ n=5, K14Ras B Cell Transfer n=10, K14Ras CD8 + B Cell Co-Transfer n=3. D: InvRas*Rag1*+/+ n=9, InvRas B Cell Transfer n=3, InvRas CD8 + B Cell Co-Transfer n=3.)

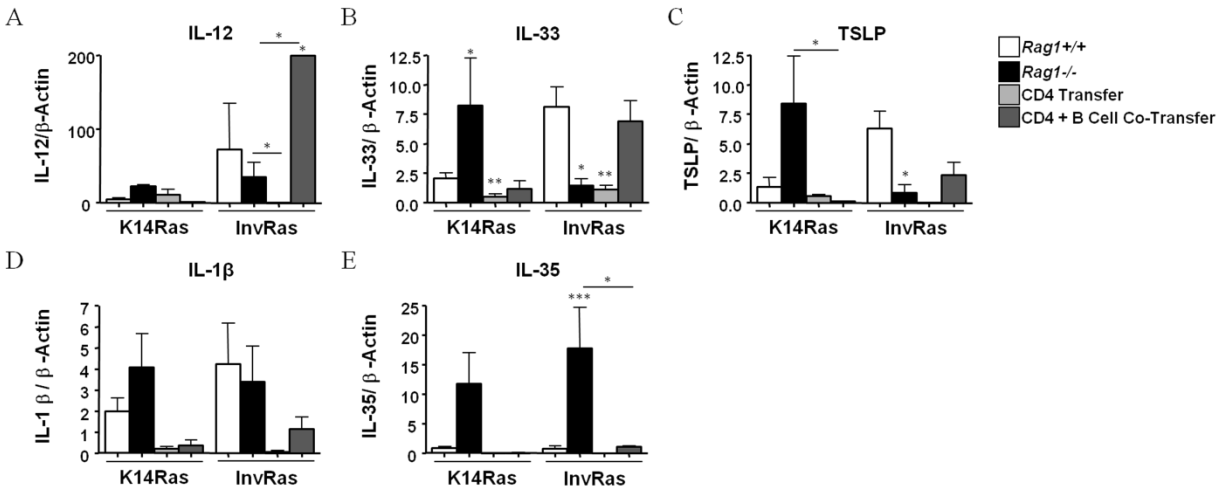


**Supplementary Figure 5:** Adoptive co-transfer of CD4 T Cells and B cells selectively restores *Rag1*+/+ cytokine expression. Relative expression of specific cytokines by qPCR in whole tumor tissue from adoptive transfer experiments examining IL-12 (A), IL-33 (B), Thymic Stromal Lymphoprotein (TSLP) (C), IL-1β (D), and IL-35 (E). Samples below detection level were not used in analysis. K14Ras*Rag1*+/+ n=15(A), 16(B), 17(C), 16(D), 16(E), K14Ras*Rag1*-/- n=4(A), 4(B), 4(C), 4(D), 4(E), K14Ras CD4 Adoptive Transfer n=8(A), 8(B), 7(C), 4(D), 3(E), K14Ras CD4 + B Cell Co-Transfer n=4(A), 8(B), 6(C), 4(D), 2(E). InvRas*Rag1*+/+ n=6(A), 12(B), 12(C), 12(D), 6(E), InvRas*Rag1*-/- n=2(A), 4(B), 3(C), 5(D), 5(E), InvRas CD4 Adoptive Transfer n=2(A), 4(B), 3(C), 2(D), 2(E), InvRas CD4 + B Cell Co-Transfer n=2(A), 6(B), 4(C), 3(D), 2(E).

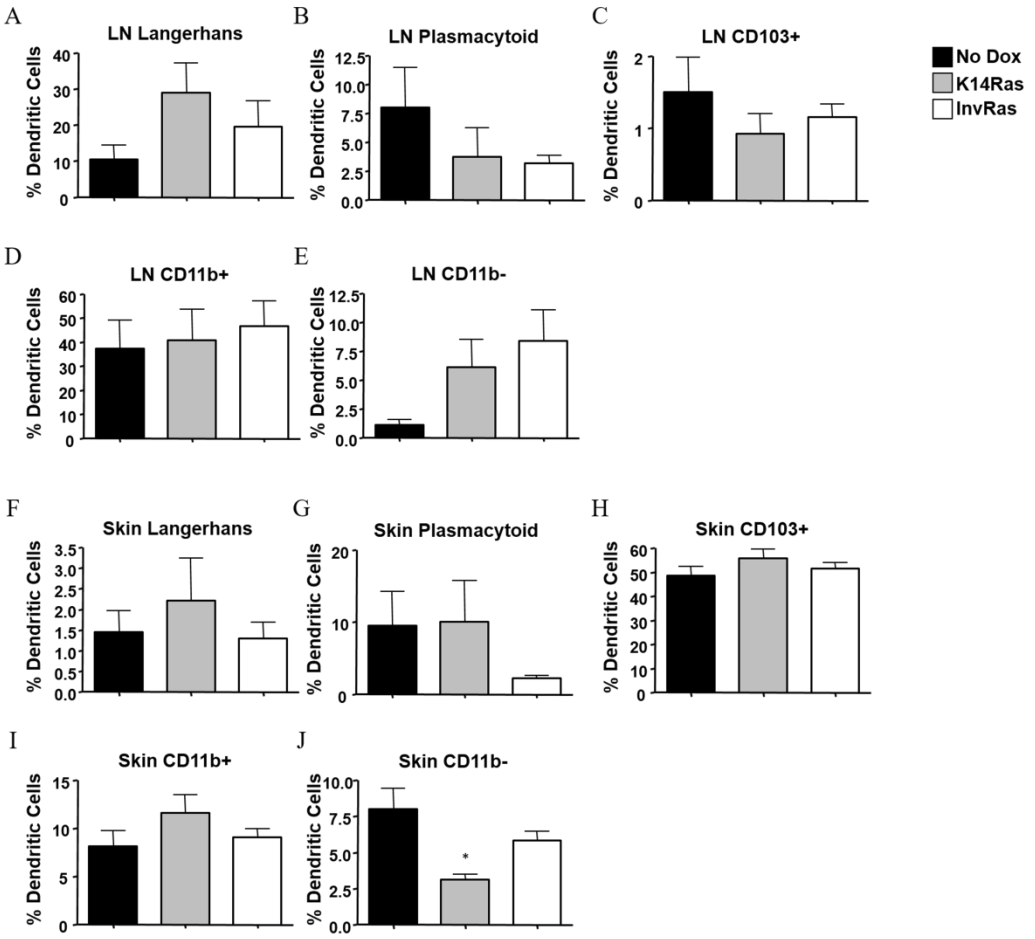


**Supplementary Figure 6:** Dendritic Cell activity in hyperplastic skin or SDLNs does not significantly contribute to the overall Ras-induced immune response. Analysis of epidermal and dermal dendritic cell subsets in inguinal lymph nodes of healthy control (No Dox) and tumor-bearing K14Ras and InvRas mice. Dendritic cell subsets analyzed include Langerhans cells (A), Plasmacytoid (B), CD103+ Dermal DCs (C), CD11b+ myeloid DCs (D), and CD11b- lymphoid DCs (E). No dox n=4, K14Ras n=4, InvRas n=5. Analysis of Langerhans cells (F), Plasmacytoid (G), CD103+ Dermal DCs (H), CD11b+ myeloid DCs (I), and CD11b- lymphoid DCs (J) in healthy skin and hyperplastic skin of K14Ras and InvRas mice. No Dox n=4, K14Ras n=4, InvRas n=6.

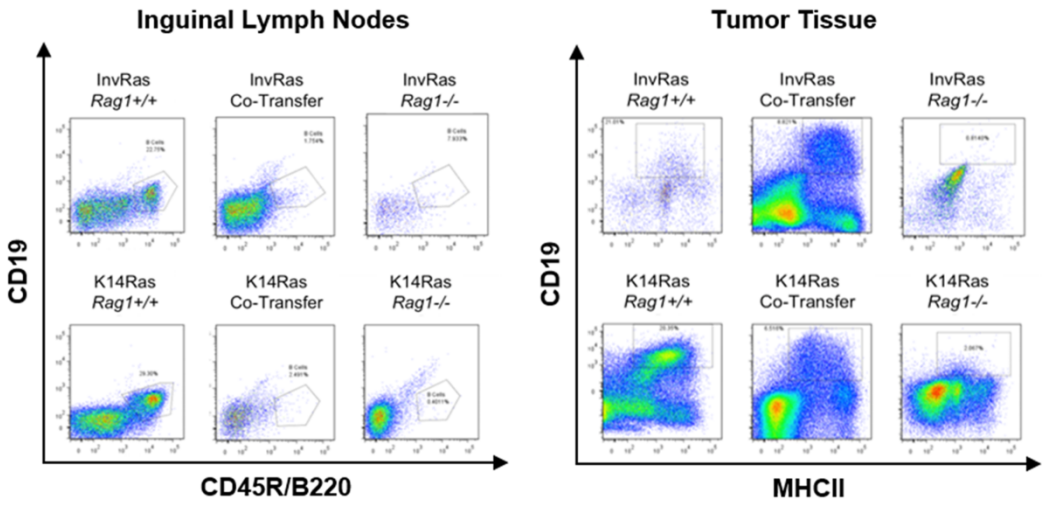


**Supplementary Figure 7:** Adoptively transferred B cells migrate directly to the tumor microenvironment following Ras activation. Representative flow cytometric analysis of inguinal lymph nodes and tumor tissue of *Rag1*+/+, *Rag1*-/-, and co-transferred mice. B cells were gated on CD19/CD45R/B220 +/+ within the CD45+, CD3- population within lymph nodes, and on CD19/MHCII +/+ within the Live CD45+ population in tumor tissue.